Electronic Supplementary Material (ESI) for Journal of Materials Chemistry A.

Supporting Information

Sandwich-like CoNiLDH@rGO@$CoNi_2S_4$ electrode enabling high mass loading and high areal capacitance for solid-state supercapacitors

Jingjing Hu, Li Sun, Feng Xie, Yaru Qu, Hankun Tan, Xiancheng Shi, Jialong Qian, Ke Wang, Yihe Zhang**

Beijing Key Laboratory of Materials Utilization of Nonmetallic Minerals and Solid Wastes, National Laboratory of Mineral Materials, School of Materials Science and Technology, China University of Geosciences, Beijing, 100083, PR China

* Corresponding authors

E-mail address: sunli@cugb.edu.cn, zyh@cugb.edu.cn

***First-principles Calculation*:** To calculate the electronic structures of CoNiLDH and $CoNi_2S_4$, first-principles calculations were carried out with the spin-polarized Generalized Gradient Approximation (GGA) by adopting the Perdew–Burke–Ernzerh (PBE) exchange-correlation parameterization to the Density Functional Theory (DFT) incorporating the LDA+U formalism using the CASTEP program. A plane-wave basis with a kinetic energy cutoff of 400.0 eV and a Monkhorst-Pack grid with a 4×4×4 k-point mesh for the Brillouin zone integration were used value of the smearing was 0.2 eV. The electronic minimization parameter of the total energy/atom convergence tolerance was 5.0×10^{-6} eV.

For the aqueous ASCs, the average weight and area of NF are 30 mg and 1 cm × 1 cm, the prepared electrode and AC were positive and negative electrodes respectively, and the negative electrode was prepared by mixing AC, carbon black and polyvinylidene fluoride (PVDF) with a mass ratio of 8:8:1. The CR2016 coin cell is sealed with a fibrous paper diaphragm and 3M KOH electrolyte.

For solid-state ASCs, PVA/KOH gel electrolyte was used. First, 1 g of PVA was dissolved in 10 mL of water and heated under vigorous stirring at 85°C for 2h to obtain a completely clear gelatinous solution, followed by the addition of 5 mL of a solution of 1 g of KOH dissolved and stirring continued. The well-dispersed clear KOH/PVA gel solution was poured into a watch glass and left for 12h to solidify the gel electrolyte into a film.

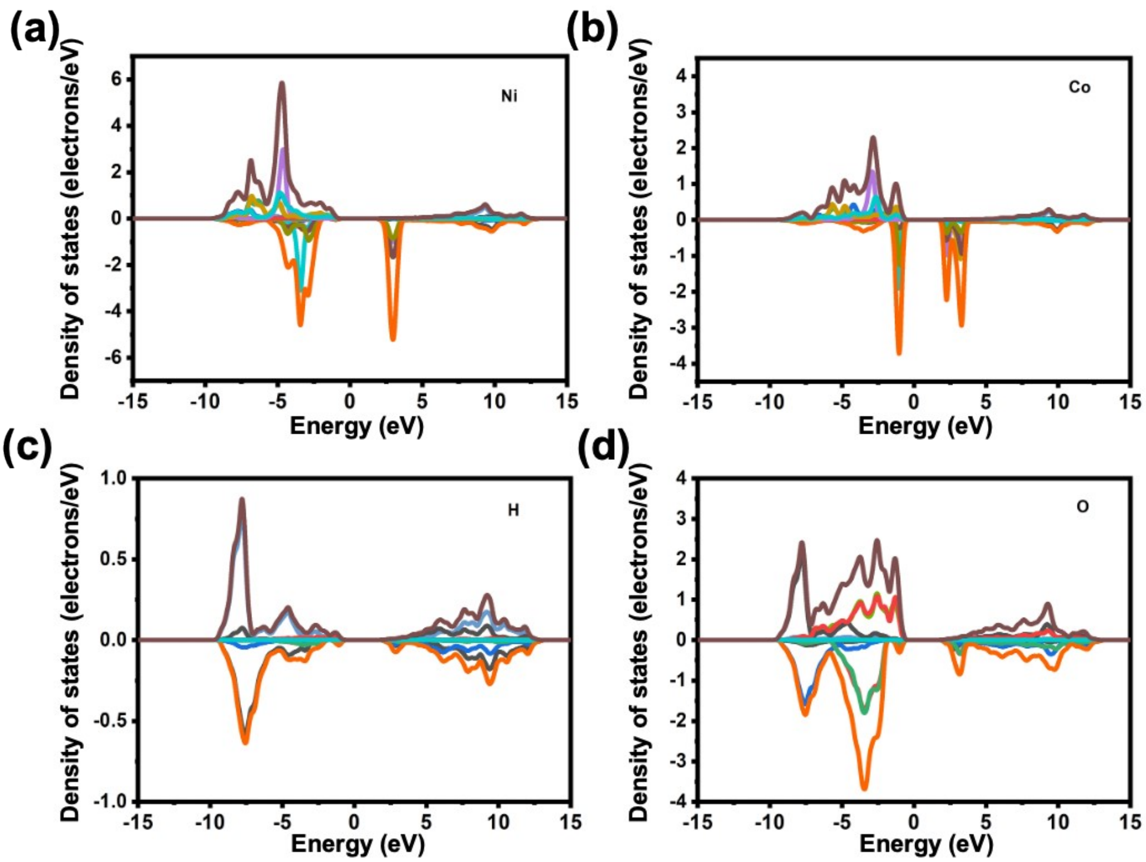

Figure S1 Projected density of states of (a) Ni (b) Co (c) H and (d) O of CoNiLDH.

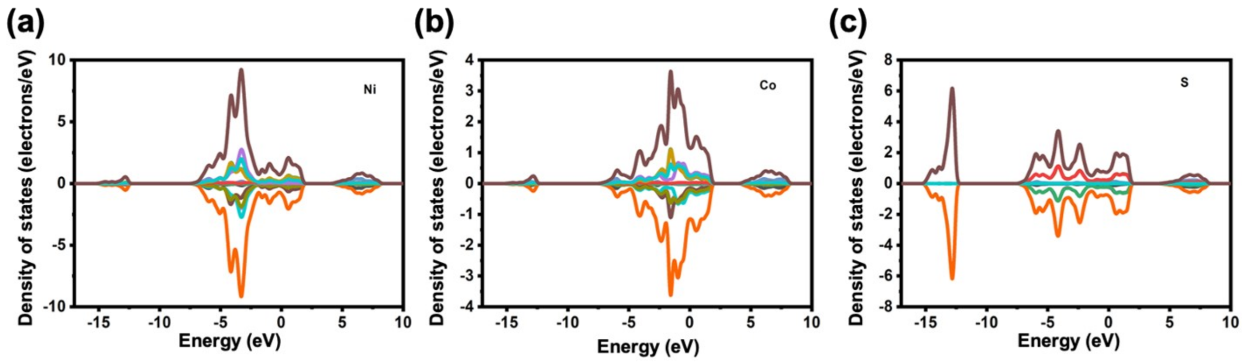

Figure S2 Projected density of states of (a) Ni (b) Co and (c) S of $CoNi_2S_4$.

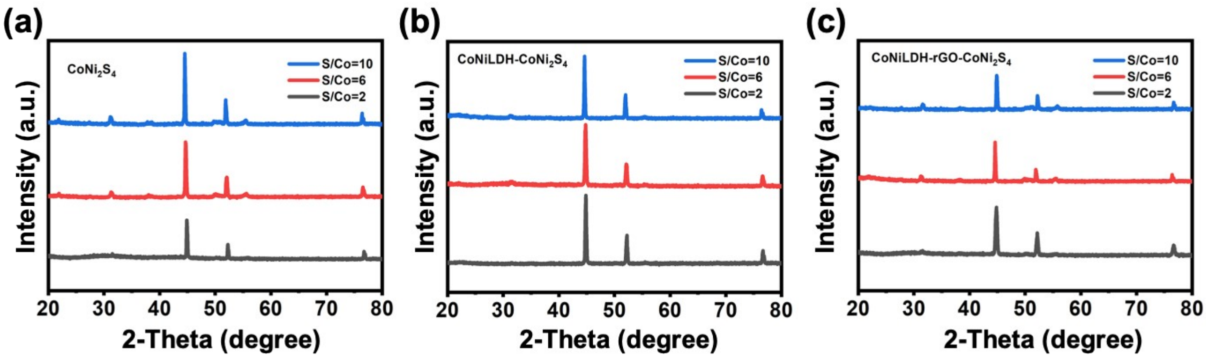

Figure S3 XRD patterns $CoNi_2S_4$, CoNiLDH-$CoNi_2S_4$, and CoNiLDH-rGO-$CoNi_2S_4$ of different S/Co ratios.

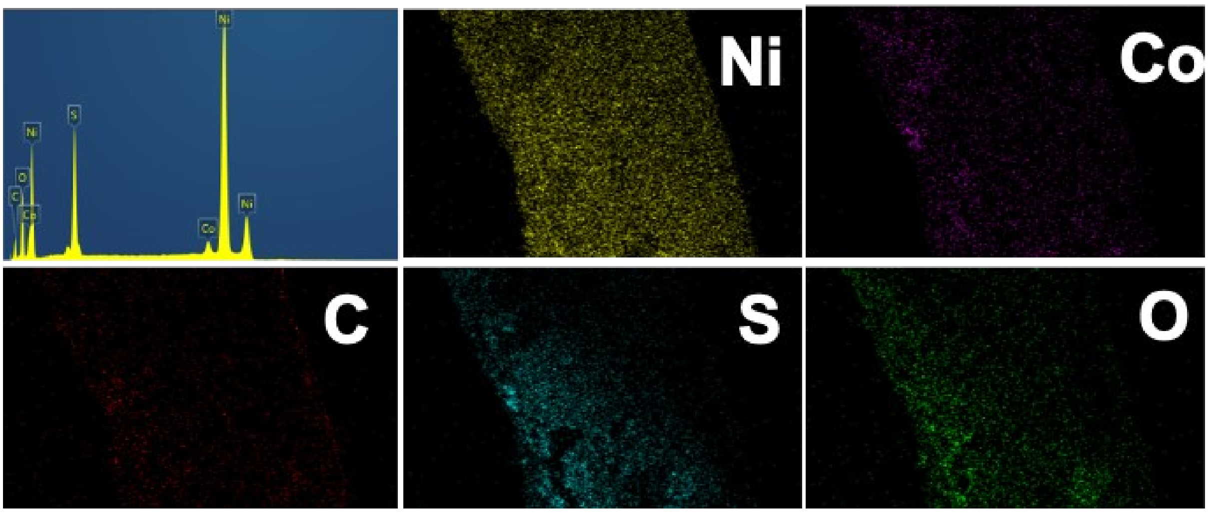

Figure S4 EDS mapping images of CoNiLDH-rGO-$CoNi_2S_4$.

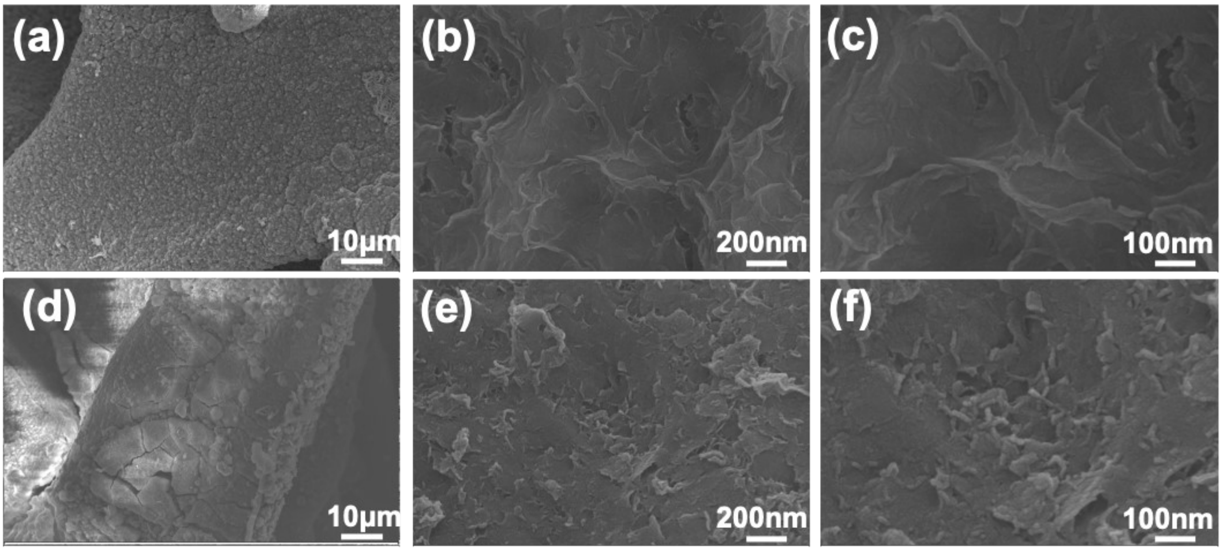

Figure S5 (a) Low-magnification and (b, c) high-magnification SEM images of CoNiLDH-rGO-$CoNi_2S_4$-6. (d) low-magnification and (e, f) high-magnification SEM images of CoNiLDH-rGO-$CoNi_2S_4$-10.

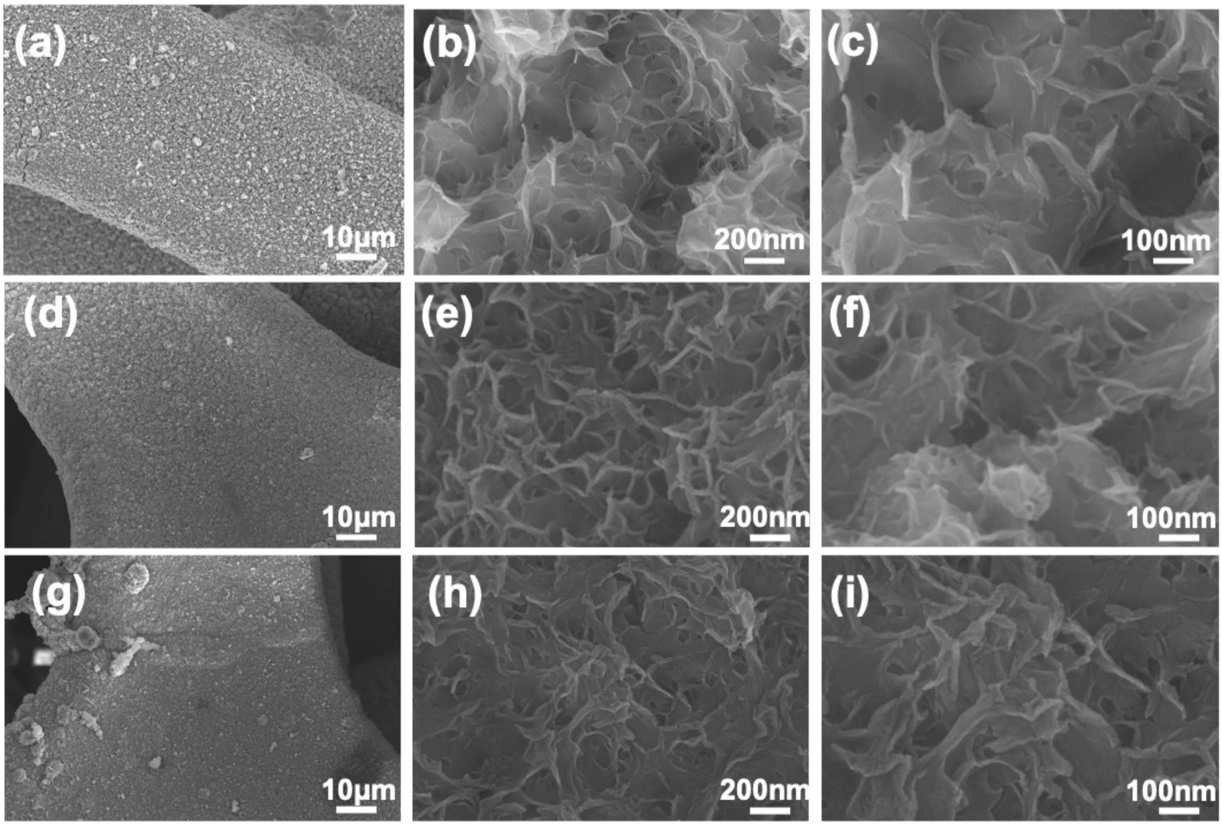

Figure S6 (a) Low-magnification and (b,c) high-magnification SEM images of $CoNi_2S_4$-2. (d) low-magnification and (e, f) high-magnification SEM images of $CoNi_2S_4$-6. (g) low-magnification and (h, i) high-magnification SEM images of $CoNi_2S_4$-10.

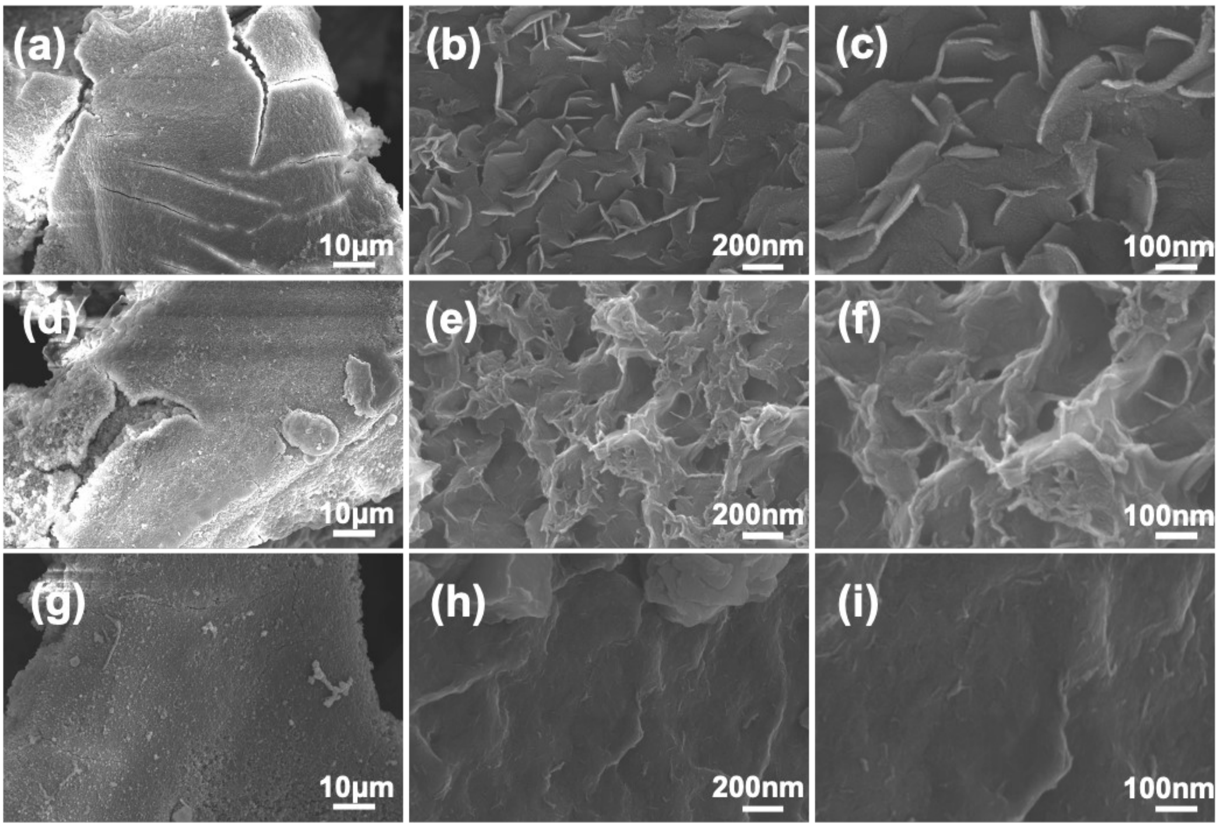

Figure S7 (a) Low-magnification and (b, c) high-magnification SEM images of CoNiLDH-$CoNi_2S_4$-2. (d) Low-magnification and (e, f) high-magnification SEM images of CoNiLDH-$CoNi_2S_4$-6. (g) low-magnification and (h, i) high-magnification SEM images of CoNiLDH-$CoNi_2S_4$-10.

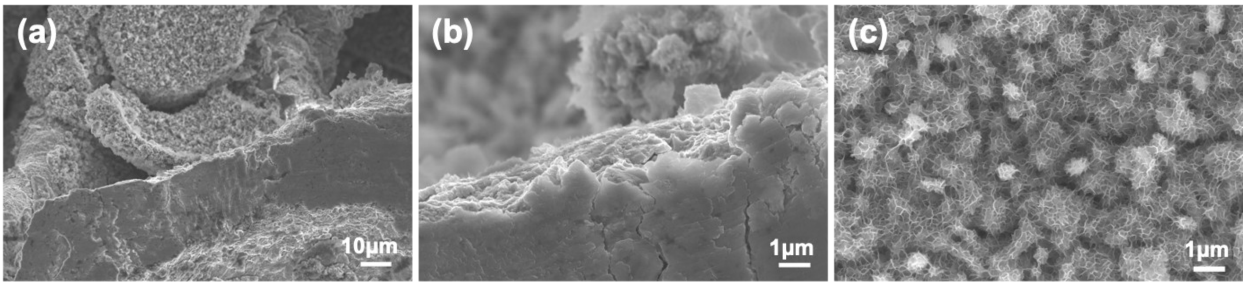

Figure S8 (a,b) Low-magnification SEM profiles and (c) plan of CoNiLDH-$CoNi_2S_4$-2.

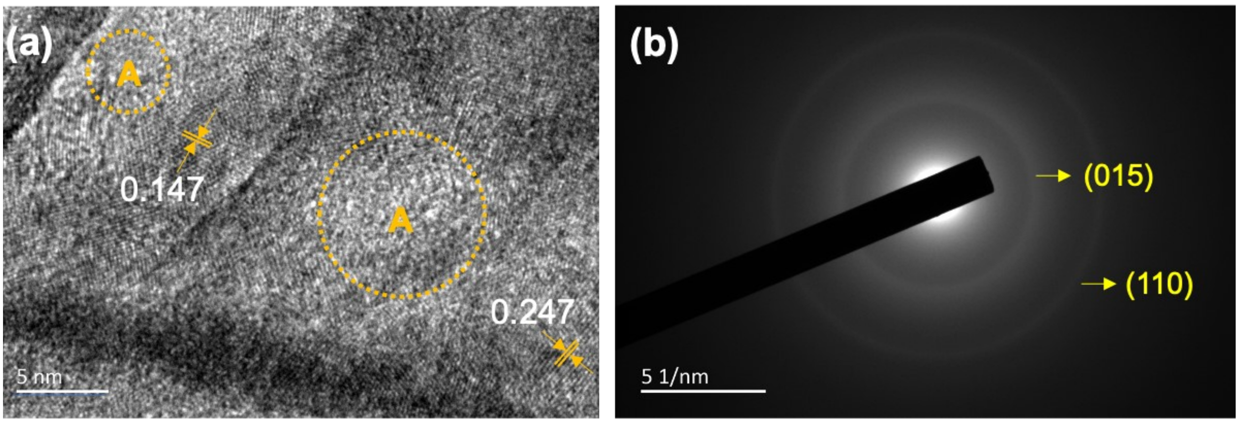

Figure S9 (a) HRTEM and (b) SAED images of CoNiLDH-rGO-$CoNi_2S_4$.

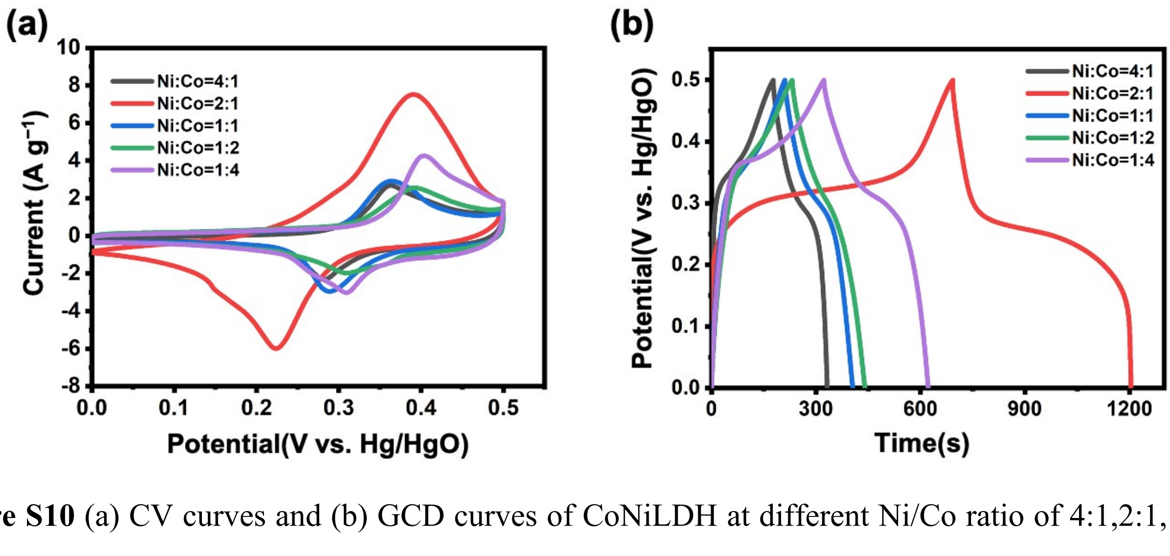

Figure S10 (a) CV curves and (b) GCD curves of CoNiLDH at different Ni/Co ratio of 4:1,2:1,1:1,1:2, and 1:4.

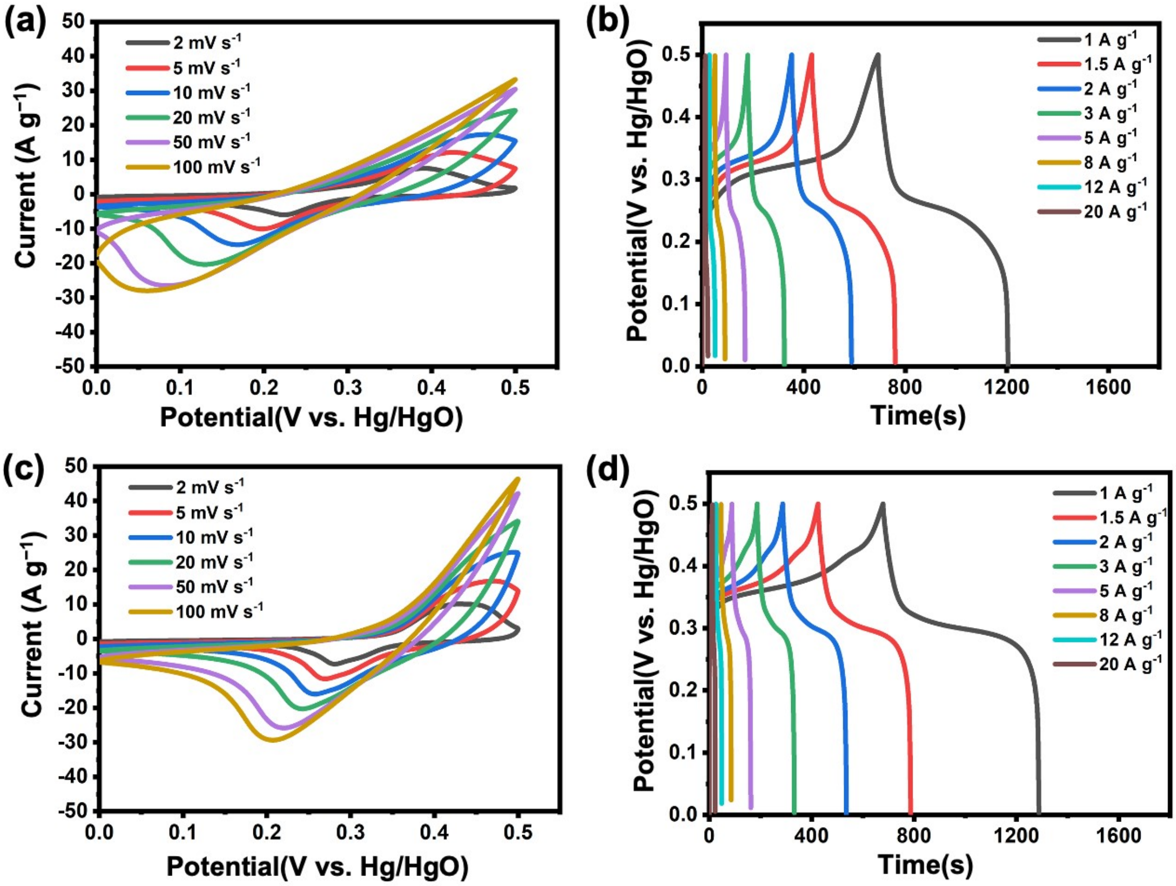

Figure S11 (a) CV curves and (b) GCD curves of CoNiLDH. (c) CV curves and (d) GCD curves of CoNiLDH-rGO.

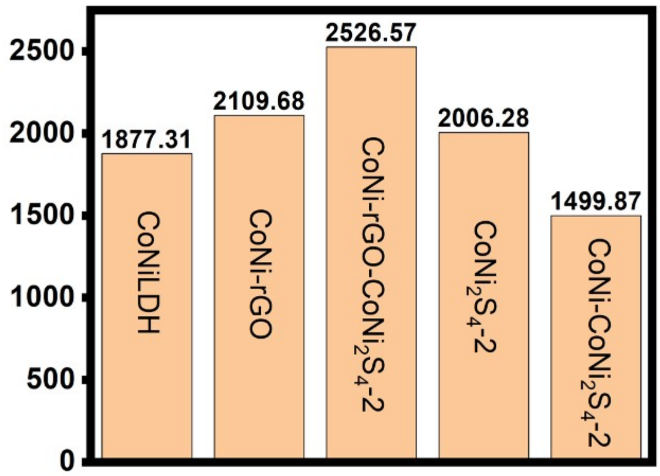

Figure S12 Mass specific capacitances of different electrodes calculated from CV curves.

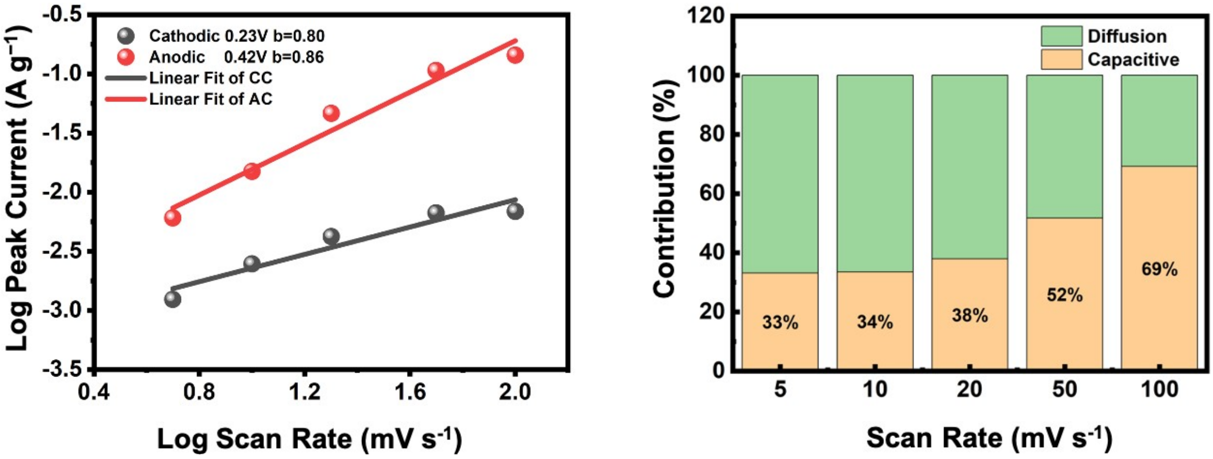

Figure S13 (a) The relationship between log(i) and log(ν) for CoNiLDH-rGO-$CoNi_2S_4$-2 electrode, (b) comparison of the capacitive contribution and diffusion contribution.

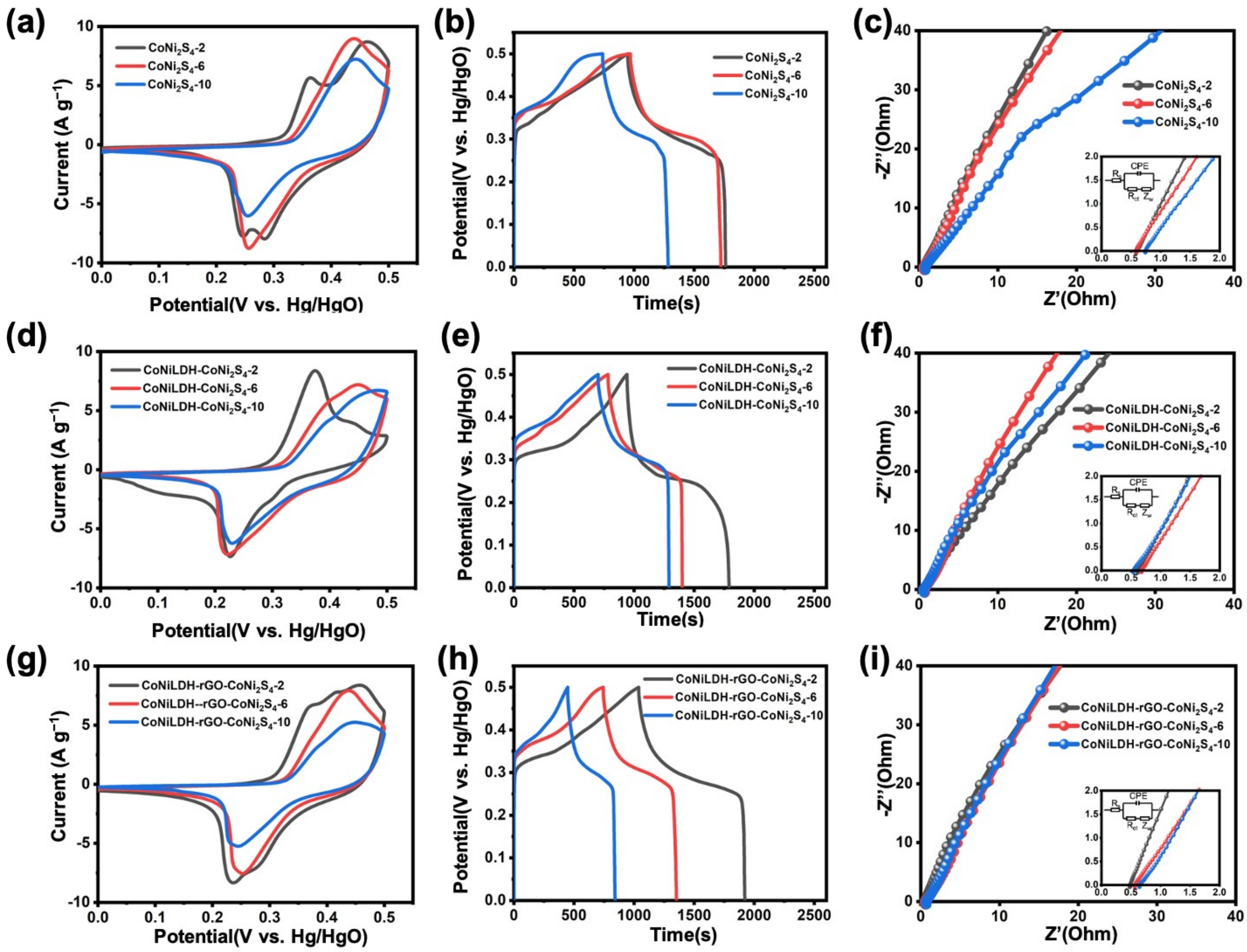

Figure S14 (a) CV curves at 2 mV s^{-1}, (b) GCD curves at 1 A g^{-1} and (c) Nyquist plots of $CoNi_2S_4$-2, $CoNi_2S_4$-6 and $CoNi_2S_4$-10. (d) CV curves at 2 mV s^{-1}, (e) GCD curves at 1 A g^{-1} and (f) EIS spectra of CoNiLDH-$CoNi_2S_4$-2, CoNiLDH-$CoNi_2S_4$-6 and CoNiLDH-$CoNi_2S_4$-10. (h) CV curves at 2 mV s^{-1}, (i) GCD curves at

1 A g^{-1} and (g) EIS spectra of CoNiLDH-rGO-$CoNi_2S_4$-2, CoNiLDH-rGO-$CoNi_2S_4$-6 and CoNiLDH-rGO-$CoNi_2S_4$-10.

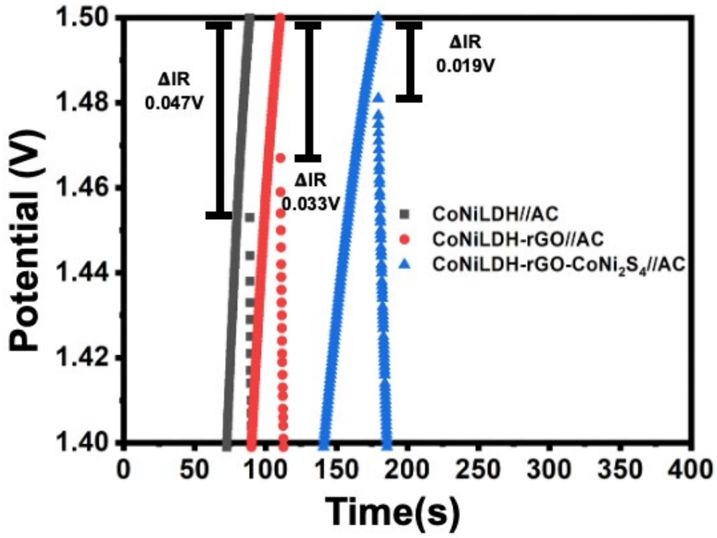

Figure S15 ΔIR drop of different ASC devices.

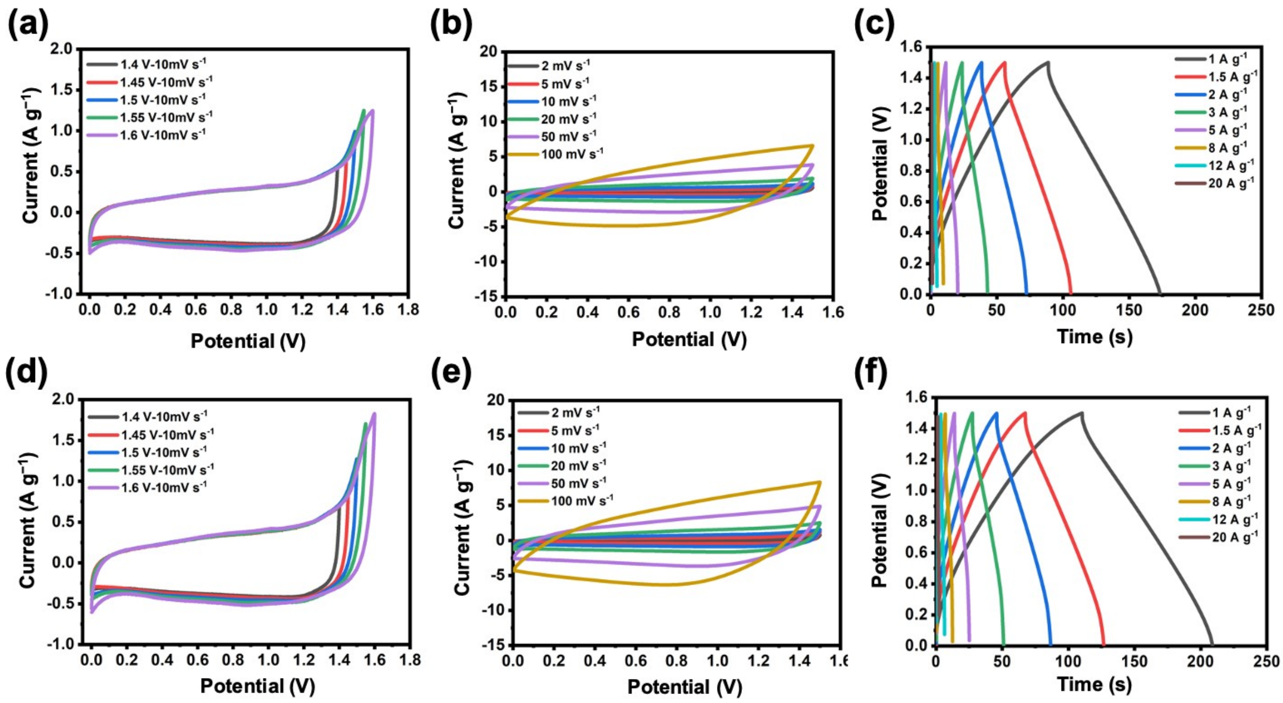

Figure S16 (a) CV curves at 10 mV s^{-1}, (b) CV curves and (c) GCD curves of CoNiLDH//AC ASC device. (d) CV curves at 10 mV s^{-1}, (e) CV curves and (f) GCD curves of CoNiLDH-rGO//AC ASC device.

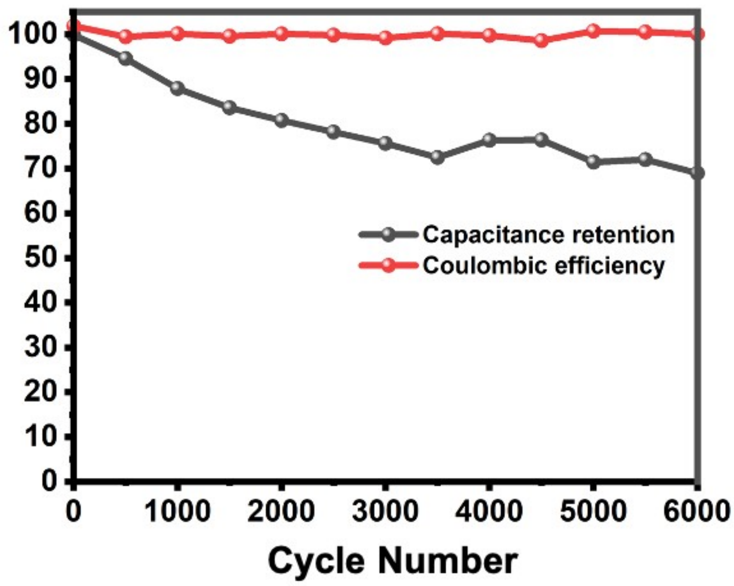

Figure S17 Long-term cycling performance and coulombic efficiency of the CoNiLDH-rGO-$CoNi_2S_4$-2//AC ASC at 3 A g^{-1} for 6 000 cycles.

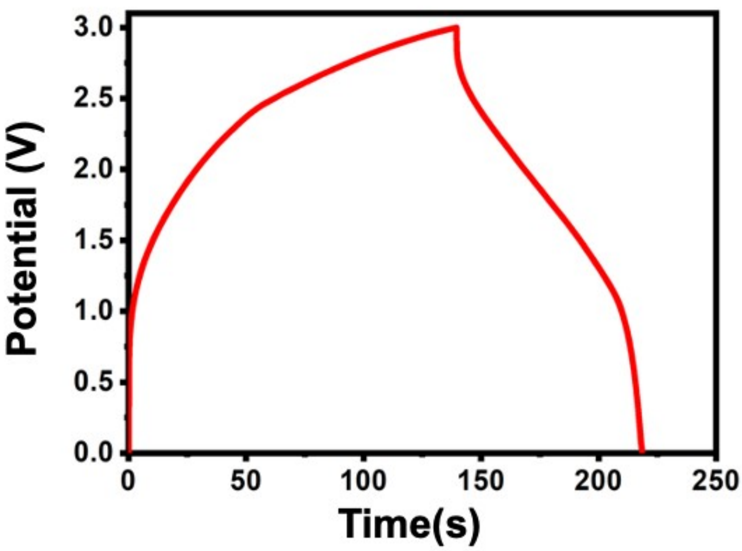

Figure S18 GCD curves at 1 A g^{-1} of CoNiLDH-rGO-$CoNi_2S_4$ //KOH+PVA//AC ASC devices in series.

Table S1. The relative contents of elements in CoNiLDH, CoNiLDH-rGO and CoNiLDH-rGO-CoNi2S4 were derived from XPS data.

Samples	Co (at.%)	Ni (at.%)	C (at.%)	S (at.%)	O (at.%)
CoNiLDH	8.75	14.94	28.97	/	47.34
CoNiLDH-rGO	3.88	6.13	56.94	/	33.05
CoNiLDH-rGO-$CoNi_2S_4$	8.68	18.95	22.77	2.37	47.24

Table S2. The R_S and R_{ct} of different electrodes.

Samples	CoNiLDH		CoNiLDH-rGO		CoNiLDH-rGO-$CoNi_2S_4$		$CoNi_2S_4$		CoNiLDH-$CoNi_2S_4$	
Ω	R_S	R_{ct}	R_S	R_{ct}	R_S	R_{ct}	R_S	R_{ct}	R_S	R_{ct}
	1.154	1.296	0.648	1.186	/		/		/	
S/Co=2	/		/		0.489	0.546	0.574	1.602	0.617	1.728
S/Co=6	/		/		0.545	0.880	0.617	3.039	0.684	1.074
S/Co=10	/		/		0.675	1.396	0.658	4.313	0.701	1.199

Table S3 Electrochemical performance of different aqueous devices.

P ($W\cdot kg^{-1}$)	E ($Wh\cdot kg^{-1}$)	Electrode material	Reference
749.9	31.60889		
1124.8	27.62667		
1499.6	25.41778	CoNiLDH-rGO-$CoNi_2S_4$//AC	This work
2249.5	22.87111		
3479.4	19.58222		
120	34.62	$NiCo_2S_4$@PPy-50/NF//AC	[1]
334/8000	25.5/9.7	$NiCo_2S_4$ nanosheets//AC	[2]
160/2470	22.8/10.6	$NiCo_2S_4$//C	[3]

245/9800	28.3/6.8	$NiCo_2S_4$//AC	[4]
334/2400	24.9/12.6	$NiCo_2S_4$ nanotube@$NiCo_2S_4$ nanosheet arrays//rGO	[5]
2461	23.9	Graphene/$NiCo_2S_4$ nanotube/$Co_yNi_{(3-x)}S_2$ nanosheets//rGO	[6]
160	38.3	NiS/NHCS//AC	[7]
885.6/1330	38.6/23.7	$CoNi_2S_4$-G-$MoSe_2$	[8]

Table S4 Electrochemical performance of different all-solid-state devices

P (W cm^{-3})	E (Wh cm^{-3})	Device	Electrolyte	Reference
32.25	1.12	CoNiLDH-rGO-$CoNi_2S_4$//AC	PVA/KOH（1.5V）	This work
31.97	1.35	CoNiLDH-rGO-$CoNi_2S_4$//AC		
23.63	0.65	CoNiLDH-rGO//AC	3M KOH（1.5V）	This work
22.45	0.53	CoNiLDH//AC		
6	1.13	MnO_2@PEDOT:PSS//OMC	CMC/Na_2SO_4	[9]
3.24	1.14	Mn_3O_4@TiO_2//MoS_2	PVA/LiCl	[10]
1.93	0.733	Ag_2O-$HMnO_2$//PANF@α-FeOOH	PVA/Na_2SO_4	[11]
3.67	1.09	$Ni(OH)_2$/MnO_2@CNT//APDC	1M KOH	[12]

[1] M. Yan, Y. Yao, J. Wen, L. Long, M. Kong, G. Zhang, X. Liao, G. Yin, Z. Huang, *ACS Appl. Mater. Interfaces* **2016**, *8*, 24525.

[2] Z. Wu, X. Pu, X. Ji, Y. Zhu, M. Jing, Q. Chen, F. Jiao, *Electrochim. Acta* **2015**, *174*, 238.

[3] W. Kong, C. Lu, W. Zhang, J. Pu, Z. Wang, *J. Mater. Chem. A* **2015**, *3*, 12452.

[4] Y. Zhu, Z. Wu, M. Jing, X. Yang, W. Song, X. Ji, *J. Power Sources* **2015**, *273*, 584.

[5] H. Chen, S. Chen, H. Shao, C. Li, M. Fan, D. Chen, G. Tian, K. Shu, *Chem. - An Asian J.* **2016**, *11*, 248.

[6] L. G. Beka, X. Li, W. Liu, *Sci. Rep.* **2017**, *7*, 1.

[7] T. Liu, C. Jiang, B. Cheng, W. You, J. Yu, *J. Mater. Chem. A* **2017**, *5*, 21257.

[8] J. Shen, J. Wu, L. Pei, M. T. F. Rodrigues, Z. Q. Zhang, F. Zhang, X. Zhang, P. M. Ajayan, M. Ye,

Adv. Energy Mater. **2016**, *6*, 1.

[9] X. Cheng, J. Zhang, J. Ren, N. Liu, P. Chen, Y. Zhang, J. Deng, Y. Wang, H. Peng, *J. Phys. Chem. C* **2016**, *120*, 9685.

[10] R. Lin, Z. Zhu, X. Yu, Y. Zhong, Z. Wang, S. Tan, C. Zhao, W. Mai, *J. Mater. Chem. A* **2017**, *5*, 814.

[11] Y. Mao, J. Xie, C. Guo, H. Liu, H. Xiao, W. Hu, *Chem. Eng. J.* **2021**, *426*, 131188.

[12] J. Shen, X. Li, L. Wan, K. Liang, B. K. Tay, L. Kong, X. Yan, *ACS Appl. Mater. Interfaces* **2017**, *9*, 668.